International Journal of Environmental Sciences
ISSN: 2229-7359
Vol. 11 No. 21s, 2025
https://theaspd.com/index.php

Impact Of Orientation On The Thermal Performance Of Building-Integrated Photovoltaic Modules In Ventilated Façades In Hot Climates

Mohammed Al-Neama[1], Sherifa Al Hayyas[2], Edwin Rodriguez-Ubinas[2], Hasan Rafiq[2], Ahmer Baloch[2]
[1]Department of Sustainable and Renewable Energy Engineering, University of Sharjah, Sharjah, UAE
[2]Dubai Electricity and Water Authority, DEWA R&D Centre, Dubai, UAE
U23103026@sharjah.ac.ae; sherifa.alhayyas@dewa.gov.ae; edwin.ubinas@dewa.gov.ae; hasan.rafiq@dewa.gov.ae; ahmer.baloch@dewa.gov.ae
*Corresponding Author: edwin.ubinas@dewa.gov.ae

***Abstract*—** *Building-integrated photovoltaic (BIPV) systems represent a promising approach for creating a sustainable built environment by incorporating photovoltaic surfaces directly into the building envelope, effectively replacing conventional construction materials and building elements. These systems can be seamlessly integrated into a variety of components, including roofs, façades, windows, and shading devices. Among the various configurations, ventilated BIPV façades are increasingly recognized for their dual role in enhancing energy efficiency and generating clean energy. Despite their growing global relevance, the thermal performance of BIPV ventilated façades, particularly their heat loss factor (U), remains insufficiently explored in extremely hot climates, such as those in the Middle East. This work aims to identify the best-fit heat loss factor for simulating the energy yield of ventilated BIPV façades in Dubai. The factor was calibrated via one year of measurements from façades facing South, East, and West. The parametric simulations were conducted via PVsyst software. The analysis reveals that the heat loss factor is influenced not only by the mounting configuration but also by the orientation. The recommended thermal loss constant for semi-integrated solutions is 20 W/m2K. However, the best-fit values for the East, South, and West façades are 13, 17, and 27 W/m^{2}K, respectively. With these values, the simulations exhibit excellent agreement with the measured energy yields, with the absolute difference and mean bias difference both below 0.3% and the root mean square difference under 5%. This study further validates the importance of calibrating the thermal parameters to the specific façade construction and climatic context, as it leads to enhanced simulation accuracy. Additionally, this study revealed that heat loss coefficients from PV modules in façades are influenced not only by wind and the free space behind them but also by the façade orientation.*

***Keywords*–** *building-integrated photovoltaics, crystalline silicon, PVsyst, solar energy, ventilated façades.*

I. INTRODUCTION

Solar energy is increasingly recognized as a viable and strategic alternative to conventional fossil fuels for electricity generation. As a clean, renewable, and environmentally sustainable source of energy, solar power offers significant potential to address the growing global energy demand while reducing greenhouse gas emissions and minimizing the environmental footprint associated with traditional energy systems. The Middle East and North Africa (MENA) regions are particularly well-positioned to benefit from solar energy because of their high levels of solar irradiance, as illustrated in Fig. 1. With an abundance of sunlight throughout the year, the region has the potential to harness this resource to produce substantial amounts of electricity.

Large-scale electricity generation requires extensive surface areas, which may not always be feasible in densely built environments. High-rise buildings, for example, have limited roof space relative to their energy consumption. As such, installing traditional PV modules solely on the rooftops of skyscrapers typically generates only a small proportion of the total building energy demand, making complete reliance on rooftop PV systems impractical for such structures. These spatial constraints highlight the need for innovative solar integration methods within the built environment. In response to these challenges, building-integrated photovoltaics (BIPVs) have emerged as promising and transformative technologies in the solar energy field. BIPV systems are designed to serve dual functions: generating electricity while simultaneously acting as part of the building envelope.

International Journal of Environmental Sciences
ISSN: 2229-7359
Vol. 11 No. 21s, 2025
https://theaspd.com/index.php

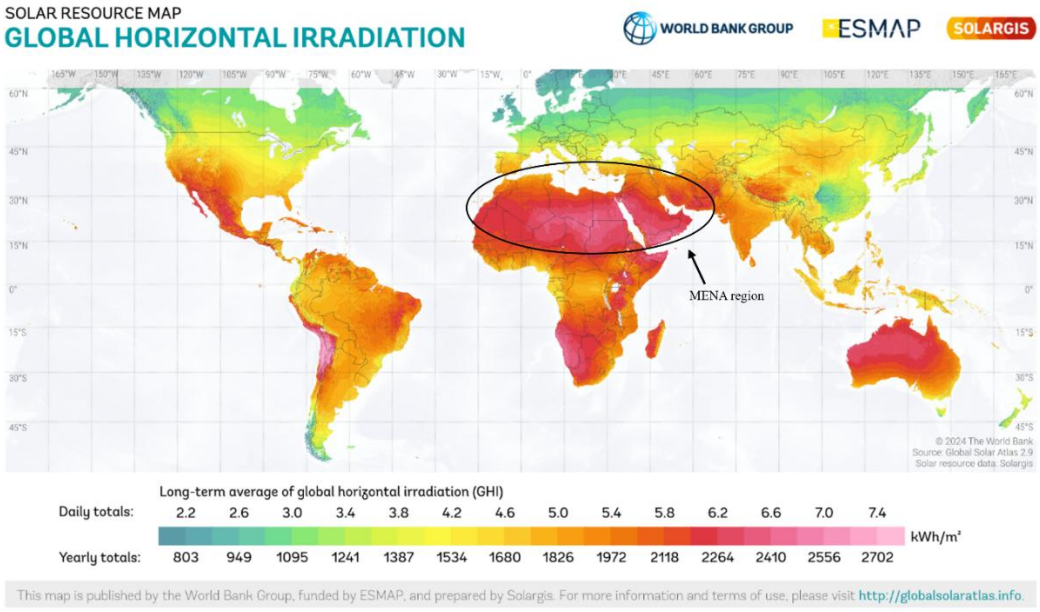

Fig. 1 Worldwide long-term average global horizontal irradiation [1].

Unlike conventional building-applied photovoltaics (BAPVs), which are retrofitted onto existing surfaces, BIPV systems are seamlessly integrated into the architectural design, replacing conventional building materials such as glass panels, concrete cladding, roof skylights, and shading elements [2]. BIPV modules can be incorporated into various parts of a building, including rooftops, façades, windows, balcony railings, and shading structures such as canopies and louvers [3,4]. This broad range of integration options allows for the maximization of the surface area dedicated to solar power generation, even in vertical and other non-traditional orientations. Furthermore, BIPV technologies offer aesthetic flexibility, with modules available in various colors, shapes, and degrees of transparency, ranging from translucent to semi-transparent and fully opaque configurations [5,6]. This design versatility enables architects and developers to achieve both functional and aesthetic goals, ultimately contributing to the development of energy-efficient, visually appealing, and environmentally responsible buildings.

The incorporation of a ventilated air gap behind PV modules facilitates convective cooling, creating a chimney effect. The airflow helps remove heat, effectively reducing module temperatures and mitigating thermal losses [7]. This cooling mechanism not only improves the electrical performance of the PV system but also extends the lifespan of the modules. Studies have demonstrated that such ventilated configurations can lead to temperature reductions, thereby increasing overall system efficiency [8]. Alhammadi et al. experimentally investigated the operation of ventilated BIPV façades facing South, East, and West. They studied two PV materials in the extremely hot climate of Dubai, UAE. They reported that in winter, south-facing modules provide the highest energy yield, whereas in summer, west- and east-facing façades produce more energy than do south-facing façades [9]. Martin-Chivelet et al. retrofitted a real building with a BIPV ventilated façade; their study also included South, East, and West façades. They reported that BIPV ventilated façades exhibit temperatures approximately 20°C lower than those of polymer concrete panels and 12°C lower than those of non-ventilated BIPV façades at the maximum power point. This drop in temperature results in 6% more power production under nominal operating conditions [8].

The PV module temperature (T_{module}) plays a significant role in the energy produced by the PV module, as does the heat loss factor (U). At higher PV temperatures, the efficiency of PV modules begins to decline [10], making T_{module} a crucial factor in estimating the energy yield of PV systems, along with U, as it directly affects T_{module}. The PV module temperature can be calculated via the following equation [11]:

$$T_{module} = T_{amb} + \frac{1}{U}(\alpha \cdot G_{inc} \cdot (1 - \eta_{PV})) \quad (1)$$

where U equals [11]:

$$U = U_c + U_v \cdot v_w \quad (2)$$

where T_{amb} is the ambient temperature (°C), α is the absorptivity of the PV module, G_{inc} is the incident solar radiation on the module in W/m^2, and η_{PV} is the efficiency of the PV module. U_c is the constant heat loss factor in W/(m^{2}K), U_v is the wind-dependent heat loss factor in W·s/(m^{3}K), and v_w is the wind speed in m/s.

Owen et al. experimentally tested PV modules with free ventilation and restricted ventilation (50-, 100-, and 150-mm air gaps) in South Africa at four different tilt angles ranging from 0° to 23°. The reported Uc ranges between 23.3 and 30.9 W/m^{2}K, whereas the Uv varies between 3.2 and 5.9 W·s/m^{3}K. They concluded that higher values of Uc and Uv are found at higher rear-side air gaps [12]. Sun et al. optimized the operation of roof-structured BIPVs by studying the air gap, panel spacing, and heating power in computational fluid dynamics (CFD) simulations. They validated their numerical model with experiments in China. They achieved a mean bias difference (MBD) of 10.24% and a root mean square difference (RMSD) of 23.97% for electricity generation [13]. Gonçalves et al. developed complex and simplified physical-based models for a BIPV-restricted ventilation curtain wall and compared their results with experimental data collected in Belgium. Their results revealed that the complex model (multi-physics) was able to achieve an average difference in the daily energy yield of 6.2% and an average rear-side temperature difference of 1.74°C. On the other hand, two simplified models (empirical temperature correlations) yielded average daily energy yields of 10.2% and 10.5% and average rear-side temperature differences of 3.5°C and 4.4°C, respectively [14]. Ghabuzyan et al. studied the effects of ambient temperature, wind speed, and wind direction on PV efficiency, module temperature, and U. Their study examined a flat roof-mounted BAPV array through experimental testing and comparison with CFD and PVsyst simulations. They concluded that ambient temperature and wind speed play a vital role in PV performance, whereas wind direction has a minor effect. Additionally, they noted that the PV array temperature varies greatly at relatively high wind speeds. They also studied the effect of the wind speed on the value of U. They compared the actual value of U, which was based on the experimental results, with the values of U from CFD and PVsyst. They reported that the CFD better matches the experimental data trend; however, PVsyst is more accurate in studying the effect of U at lower wind speeds (1-4 m/s) [15]. Martín-Chivelet et al. assessed two thermal models for BIPV applications in Spain. They reported a Uc of 69.4 W/m^{2}K for the free-ventilated BIPV façade, 39.9 W/m^{2}K for restricted ventilation, and 28.7 W/m^{2}K for the non-ventilated BIPV façade, following the Faiman model. The Uv varies between 0.97 and 2.93 W·s/m^{3}K [16]. Barykina and Hammer defined the Uc and Uv for outdoor PV modules on the basis of six-month measurements at five different site locations (Germany, Italy, India, Saudi Arabia, and the United States). The reported Uc varies between 30.14 and 41.86 W/m^{2}K, and the Uv varies between 3.06 and 8.22 W·s/m^{3}K [17].

The accuracy and reliability of photovoltaic simulation tools are critical for predicting system performance, informing design decisions, and evaluating the feasibility of solar energy projects. Among these tools, PVsyst is widely used by researchers and engineers for modeling PV systems under various environmental and operational conditions. PVsyst is a design and simulation software for PV systems [18]. It is a standalone PV tool that supports the import of 3D models from other tools, such as Sketchup, Rhino [3], and Revit [19]. It supports inputting detailed specifications via PAN files (for PV modules) and OND files (for inverters) [3]. PVsyst supports the simulation of BIPV on façades [20,21] and rooftops [2]. Moreover, PVsyst enables the simulation of various ventilation scenarios for BIPV systems, including free-, restricted-, and non-ventilated conditions. It also accounts for shading losses, ensuring precise performance analysis [22,23]. Additionally, PVsyst supports opaque and semi-transparent BIPV modules [24]. PVsyst encompasses various PV materials, including monocrystalline silicon, polycrystalline silicon, and thin films. It can calculate the operating temperature of BIPV modules, offering indirect insight into potential building temperature effects [25]. Furthermore, PVsyst provides estimations of lifetime CO_2 emission reductions and system cost evaluations for BIPV installations [21]. Numerous validation studies have been conducted to assess the alignment of PVsyst simulation outputs with empirical data obtained from real-world installations. Gomes et al. validated PVsyst simulation results with experiments in Brazil. Their simulated daily energy production differs from the experimental results by between 1.3% and 30% [20]. Quddus et al. compared a 38.4 kW rooftop PV system with PVsyst simulation results for the same system and reported a 9.2% difference based on the annual average over three years. Additionally, the monthly difference between the actual and simulated results varies between 4.7% and 38.6% [2]. Zomer et al. simulated multiple real BIPV applications on different types of surfaces and compared their results with

actual data. Their results revealed that the difference in yearly energy production varies between 2% and 12% [22].

Research on BIPV ventilated façade simulations lacks information about the thermal loss factor (U) that best matches cases in extremely hot climates, such as the Gulf region; engineers and researchers often use software default values of U. Additionally, to the best of the authors' knowledge, no prior work has investigated the effect of module orientation on the thermal loss factor of PVs in façades. Therefore, this work aims to identify the optimal heat loss factor (U) for simulating the energy yield of PV modules integrated into rear-ventilated BIPV façades, utilizing onsite measurements from three façades of a building in Dubai, UAE.

II. METHODS

The experimental work was conducted on a BIPV ventilated façade of a test facility known as the BIPV Cube at the Dubai Electricity and Water Authority (DEWA) R&D Centre, which is situated in the Mohammed Bin Rashid Al Maktoum Solar Park in Dubai. It has 28 PV modules on each of its three active façades (South, East, and West). The Cube envelope features an open-joint, rear-ventilated façade, and an 8.3 cm ventilation gap separates the panels from the building thermal envelope, as illustrated in Fig. 2. The temperature and energy yield of the crystalline silicon (c-Si) modules were collected via PT-100 sensors, and the electronic loads were separated. The modules' information is presented in TABLE I.

In addition to the PV modules, the weather was tracked for a year, from April 2022 to March 2023. The weather data include solar radiation (both global and diffuse), ambient temperature, and wind speed and direction. Fig. 3 shows the monthly global horizontal irradiance (GHI), monthly diffuse horizontal irradiance (DHI), and monthly average ambient temperature (T_Amb) for the monitored period. Fig. 4 shows the wind direction for the same period at 10 m above ground from 8:00 to 17:00.

A parametric study was conducted to determine the best fit of U that yields the closest agreement between simulated and experimentally measured energy production, thereby improving the accuracy of energy yield simulations and enhancing alignment with real-world performance. The simulation of BIPV modules was conducted via PVsyst software. In this software, the default thermal loss factor (U), also referred to as the overall heat transfer coefficient, is set at 20 W/(m²·K) for configurations classified as "semi-integrated with an air duct behind", representing restricted ventilation conditions [11].

Fig. 2 The Cube facility at DEWA R&D Centre [9].

TABLE I SPECIFICATIONS OF THE C-SI MODULES.

Material	Mono c-Si	**V_{oc} (V)**	27.7
Size (m)	1.2 × 1.0	**V_{mpp} (V)**	22.9
Rated Power (W)	185	**Temp. Coeff.** (%/°C)	-0.43
I_{sc} (A)	8.7	**Efficiency** (%)	15.42
I_{mpp} (A)	8.1	**Module Area (m^2)**	1.2

International Journal of Environmental Sciences
ISSN: 2229-7359
Vol. 11 No. 21s, 2025
https://theaspd.com/index.php

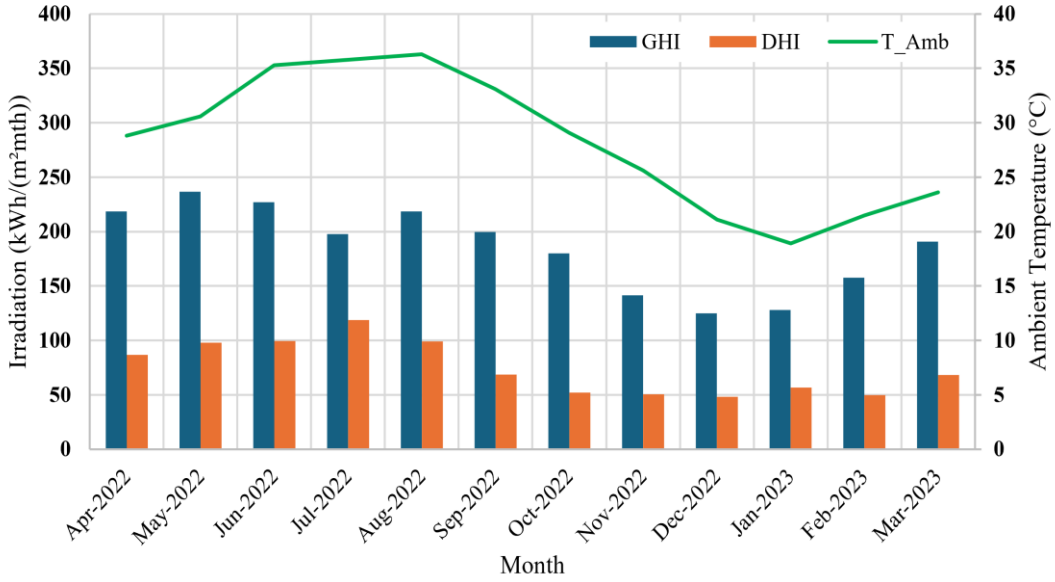

Fig. 3 Monthly GHI, DHI, and monthly average ambient temperature.

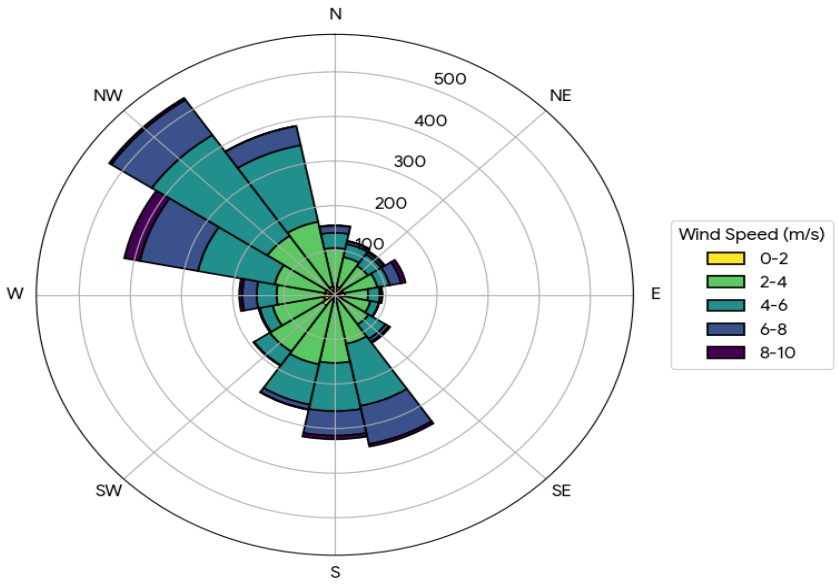

Fig. 4 Wind direction.

While this default value serves as a general baseline, it does not necessarily reflect the actual thermal behavior of all BIPV installations, particularly when factors such as façade orientation, ventilation characteristics, and climatic conditions are considered. For this purpose, a series of simulations were conducted in PVsyst using the monitored weather data, varying U from 10-45 W/(m²·K) for each façade. The simulation results were compared with the actual monitored energy yield.

Fig. 5 presents the current–voltage (I–V) characteristics of the c-Si module generated via PVsyst. This curve was generated under a standardized irradiance level of 800 W/m². The I–V profiles illustrate the electrical behavior of the module under realistic operating conditions, taking into account various loss factors. Among the key losses depicted are thermal losses due to elevated module temperatures, incidence angle modifier (IAM) losses resulting from suboptimal tilt angles, and quality-related losses inherent to the manufacturing precision and material uniformity of the PV module. The curves serve to highlight how these losses influence the output performance.

The PVsyst module temperature model is derived from the Faiman module temperature model [26], a widely recognized empirical approach in PV performance modeling. PVsyst calculates T_{module} via Equation (1). The absorptivity of the PV module is set at the default value of 0.9 during this study. Additionally, Uv is kept at zero during this study.

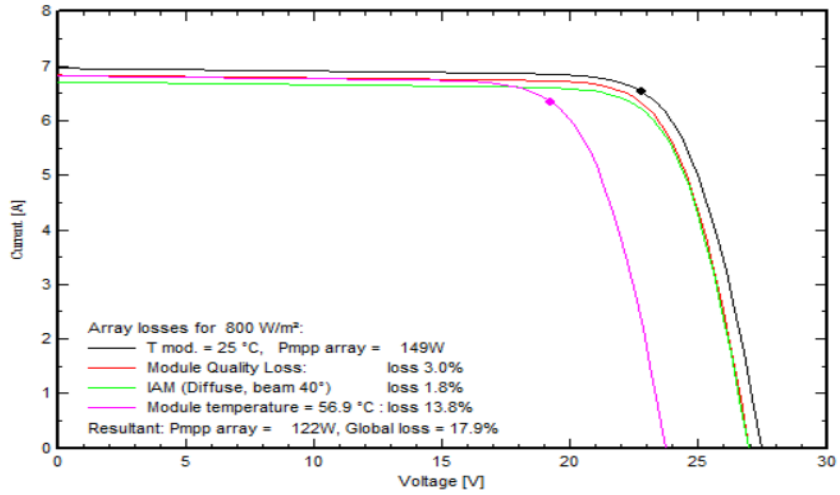

Fig. 5 I–V characteristics of the c-Si module generated via PVsyst.

The effect of the wind was neglected because the wind speed measurements taken 10 m above the ground do not reflect the actual wind conditions at the Cube. The Cube is surrounded by other objects and test facilities, which significantly minimize the effect of the wind. However, these objects and test facilities do not cause shading on the Cube.

To compare the simulated energy yield with the experimental (actual) energy yield, three metrics are utilized. These include the absolute difference (**Abs. Diff**), mean bias difference (**MBD**), and root mean square difference (**RMSD**). They are calculated via the following equations [13]:

$$\%\mathrm{MBD} = \frac{\frac{1}{\mathrm{N}}\sum_{i=1}^{\mathrm{N}}(\mathrm{EY_{act}} - \mathrm{EY_{sim}})}{\frac{1}{\mathrm{N}}\sum_{i=1}^{\mathrm{N}}(\mathrm{EY_{act}})} \times 100 \quad (3)$$

$$\%\mathrm{RMSD} = \frac{\sqrt{\frac{1}{\mathrm{N}}\sum_{i=1}^{\mathrm{N}}(\mathrm{EY_{act}} - \mathrm{EY_{sim}})^2}}{\frac{1}{\mathrm{N}}\sum_{i=1}^{\mathrm{N}}(\mathrm{EY_{act}})} \times 100 \quad (4)$$

$$\%\mathrm{Abs.\,Diff.} = \frac{|\mathrm{EY_{act}} - \mathrm{EY_{sim}}|}{\mathrm{EY_{act}}} \times 100 \quad (5)$$

where $\mathrm{EY_{sim}}$ and $\mathrm{EY_{act}}$ are the simulated and actual energy yields in kWh/m^2, respectively. **N** is the number of readings. In the current case, **N** is equal to 12 since **MBD** and **RMSD** are calculated on the basis of the monthly energy yield.

III. RESULTS AND DISCUSSION

The energy yield obtained from the PVsyst simulation was systematically compared with the experimental data via three quantitative metrics: absolute difference, RMSD, and MBD. This comparative analysis was conducted to evaluate the accuracy of the simulation model and to determine the optimal values of Uc under different conditions.

Before working on the identification of Uc for the three façades, the authors sought to gain a better understanding of the thermal behavior of the three different orientations, considering the variation in their solar radiation exposure. For the east- and west-facing façades, the pre-evaluation was carried out on the basis of the time of day. This approach was selected because variations in solar angles throughout the year have a relatively limited impact on the performance of these orientations. Consequently, the focus was placed on diurnal variations, specifically during the morning (08:00-12:00) and afternoon hours (13:00-17:00). On the other hand, the south-facing façade was analyzed with respect to seasonal changes, as it is more directly influenced by the sun's elevation and solar angles throughout the year. The symmetry in solar exposure between the morning and afternoon periods in the southern orientation further justified a seasonal rather than a temporal breakdown. The seasonal classification adopted in this study is as follows:

summer (May-July), winter (November-January), spring (February-April), and fall (August-October). Furthermore, to facilitate a holistic understanding, a full-year analysis was performed over the daily operational period (08:00-17:00). Fig. 6 summarizes the optimum Uc for each case, which is derived on the basis of the most favorable performance indicated by the evaluation metrics. The rationale behind conducting time- and season-based assessments is to gain insights into the thermal behavior of PV modules under various climatic and temporal conditions. However, for practical implementation within simulation settings, a single representative Uc is selected for each façade on the basis of its full-year performance (Fig. 7) to simplify the modeling process while maintaining accuracy.

It is important to highlight that the "West Morning" and "South Summer" cases exhibit atypical patterns. Specifically, increasing the Uc results in simulated energy yields that are marginally closer to the experimental measurements. However, the improvements observed are minimal, with only slight incremental gains. Moreover, this variation in Uc has a negligible effect on the overall model accuracy. In both cases, selecting any Uc within the tested range results in a difference of less than 1% in energy yield predictions, indicating that the simulation is relatively insensitive to this parameter under these specific conditions.

Fig. 8(a) and Fig. 8(b) show the distributions of experimentally measured BIPV module temperatures across three façade orientations (West, South, and East) under different temporal conditions: by time of day (morning vs afternoon) and by season (summer vs winter), respectively. These visualizations provide valuable thermal insights that contextualize the energy yield analysis and support the observed simulation behavior in relation to Uc.

In Fig. 8(a), which compares the morning and afternoon periods, the western façade has the highest module temperatures during the afternoon. This rise is evident in the median value and the broader interquartile range, indicating increased solar exposure later in the day. This aligns with the previously noted anomaly, where increasing Uc slightly improves the match between the simulated and experimental results, although the effect on accuracy remains marginal (less than 1%). This could be attributed to a saturation effect, where rear ventilation offers diminishing returns in thermal reduction under intense afternoon irradiance. The southern façade exhibits relatively symmetric temperature distributions between the morning and afternoon, reinforcing the decision to evaluate its performance primarily on a seasonal rather than diurnal basis. Given the consistent solar exposure throughout the day, the impact of the sun angle is more pronounced across seasons than between the morning and afternoon. This thermal consistency validates the approach of selecting a single optimal Uc on the basis of seasonal performance in the southern orientation. The eastern façade, as expected, shows higher temperatures in the morning, when solar irradiance is at its strongest. The decline in temperatures during the afternoon reflects its reduced exposure to direct sunlight.

Fig. 8(b) focuses on seasonal variation, contrasting summer and winter module temperatures. As anticipated, all orientations display elevated temperatures during the summer, driven by higher ambient temperatures and solar irradiance. The southern façade presents the most significant seasonal temperature differential, highlighting the relevance of the seasonal solar geometry to energy performance. This finding supports the earlier decision to analyze the southern façade's behavior by season, as the angle and duration of solar incidence vary significantly throughout the year.

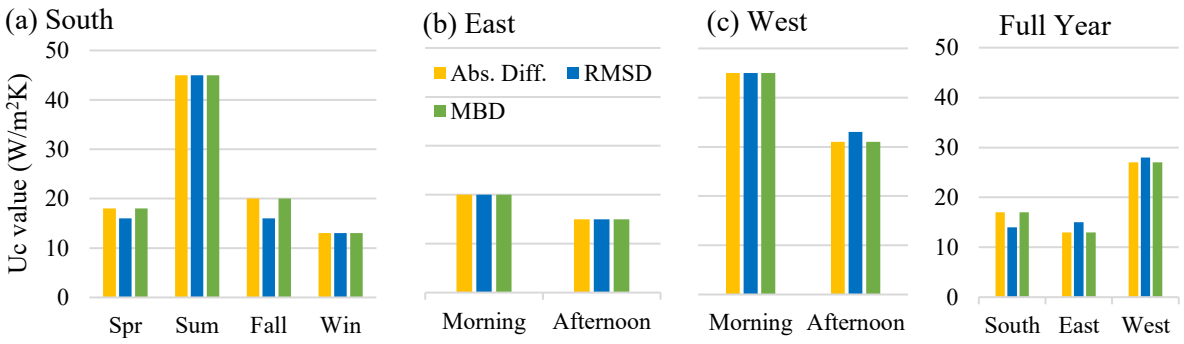

Fig. 6 Uc values provide the best fit to each condition at the three orientations.

Fig. 7 Best-fit Uc value based on the

International Journal of Environmental Sciences
ISSN: 2229-7359
Vol. 11 No. 21s, 2025
https://theaspd.com/index.php

full year (8:00 to 17:00).

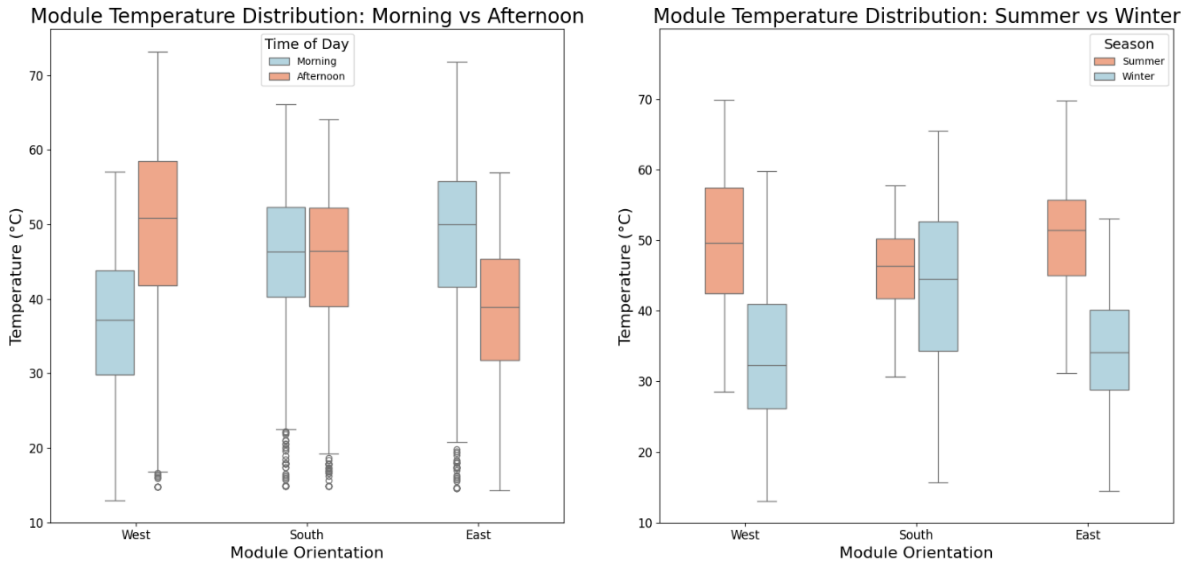

Fig. 8 Module temperature distributions (a) morning vs afternoon and (b) summer vs winter.

For the western and eastern façades, the summer temperatures are consistently higher, but the interquartile ranges suggest reduced variability compared with that in the winter, possibly due to more stable irradiance conditions. This further substantiates the approach of assessing lateral façades by time of day, where the solar angle and exposure timing play a more dominant role than do seasonal differences.

Fig. 9 presents the comparison between the monthly experimental and simulated energy yields for the South, East, and West façades. The simulations were conducted via the optimal values of Uc identified through full-year analysis between 08:00 and 17:00, which resulted in Uc values of 17 W/m²·K for the southern façade, 13 W/m²·K for the eastern façade, and 27 W/m²·K for the western façade. These values were selected to minimize the deviation between the simulated and measured data, offering the most representative thermal behavior across the year for each orientation.

Following the selection of the optimum values of Uc for each façade orientation, TABLE II summarizes the corresponding statistical indicators: absolute difference, RMSD, and MBD. The absolute difference is calculated on the basis of the annual energy yield, whereas the RMSD and MBD are calculated on the basis of the monthly energy yields. The results demonstrate excellent agreement between the simulated and experimental energy yields, with the absolute difference and MBD both remaining below 0.3% and the RMSD falling under 5%.

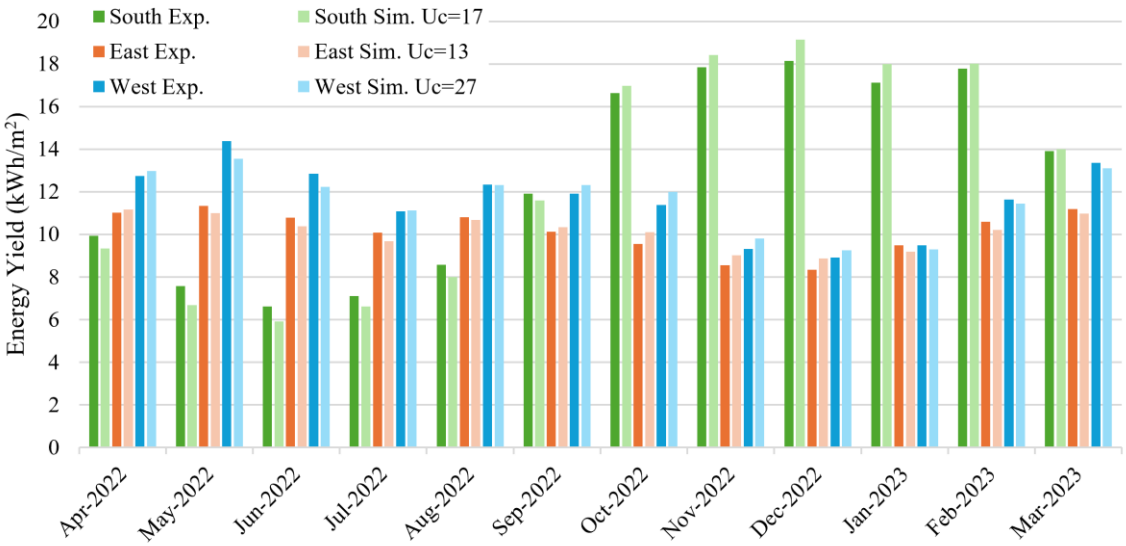

Fig. 9 Monthly experimental vs. simulated energy yields for all orientations.

TABLE II ABSOLUTE DIFFERENCE, RMSD, AND MBD OF EY AT THE OPTIMUM UC VALUES FOR EACH ORIENTATION.

Full year (8 am - 5 pm)	South		East		West	
Uc (W/m²·K)	Uc=17	Uc=20	Uc=13	Uc=20	Uc=27	Uc=20
%Abs. Diff.	0.30%	1.39%	0.15%	4.32%	0.02%	2.13%
%RMSD	4.83%	6.14%	3.59%	5.17%	3.64%	4.39%
%MBD	0.30%	1.39%	0.15%	4.32%	0.02%	2.13%

These outcomes are particularly encouraging, indicating a high level of model accuracy. Moreover, the results compare favorably with those reported in the literature and the introduction section of this study, where similar analyses by other researchers exhibited larger deviations [2,13,20,22]. This highlights the robustness of the selected values of Uc and the reliability of the simulation methodology employed. Additionally, TABLE II presents the values of the evaluation metrics when the default Uc provided by PVsyst software is used, which is 20 W/m²·K. The difference in annual energy yield between the default Uc (20 W/m²·K) and the experimental results is 1.39% for South façades, 4.32% for East façades, and 2.13% for West façades. However, the difference in annual energy yield between the best-fit Uc and the experimental results is 0.3% for South façades, 0.15% for East façades, and 0.02% for West façades. A clear and consistent improvement in model performance is observed when these default results are compared with those derived from the best-fit Uc established in this study. This comparison further validates the importance of calibrating the value of U to the specific façade orientation and climatic context, as it leads to significantly enhanced simulation accuracy.

Fig. 10 shows the comparison between the experimental and simulated energy yields on December 20 and July 24 for the south-, east-, and west-facing façades, using their respective best-fit values of Uc. The simulated results closely align with the experimental data, demonstrating strong agreement and validating the accuracy and reliability of the developed model under both winter and summer conditions. This further reinforces the model's ability to capture seasonal variations in energy yield across different orientations.

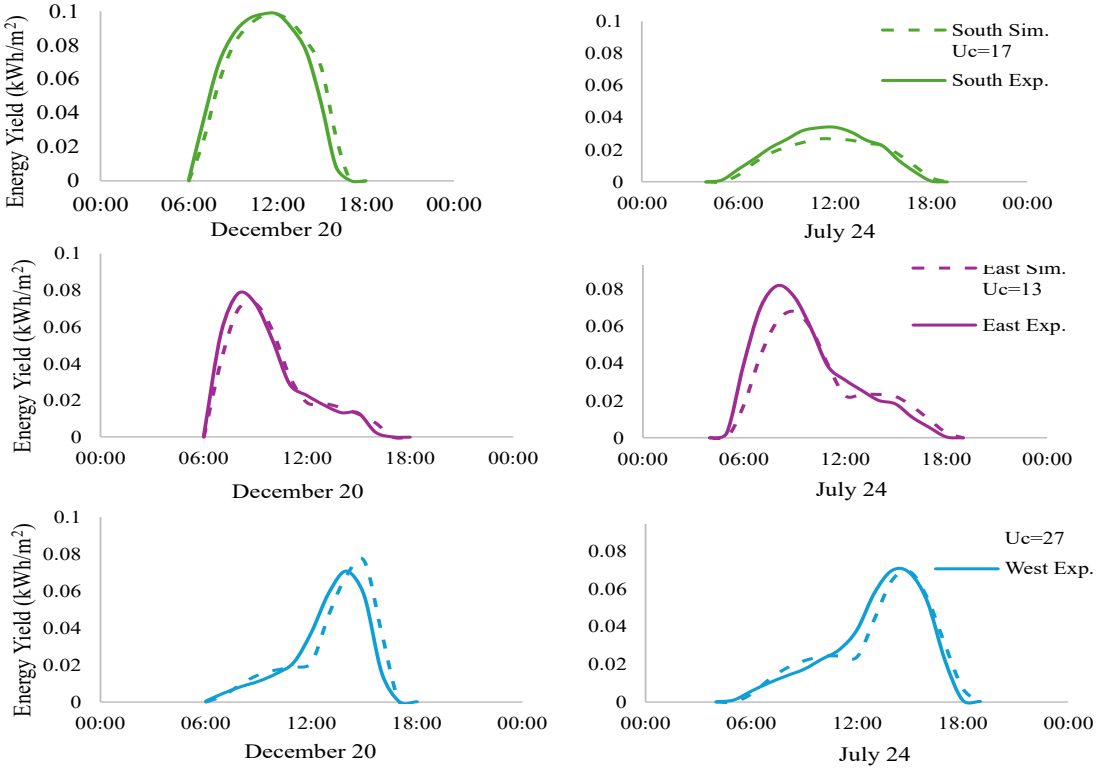

Fig. 10 Experimental vs. simulated energy yields on December 20 and July 24 for South, East, and West.

IV. CONCLUSIONS

This research addresses significant shortcomings in the simulation and performance assessment of the heat loss factor (U) in rear-ventilated BIPV façades in extremely hot climates. This research employs detailed parametric simulations with PVsyst, utilizes monocrystalline silicon BIPV modules, and verifies the results against experimental data.

The optimal values of U for the simulation of this type of BIPV façade in hot climates do not match the software default values. A relevant contribution not reported in the literature is that the optimal U for ventilated BIPV façades varies significantly with orientation. In the studied case, the optimal values of the constant heat loss factor (Uc) identified were 13 W/m²K for east-facing façades, 17 W/m²K for south-facing façades, and 27 W/m²K for west-facing façades. These findings highlight the need to move beyond default simulation parameters to account for orientation-dependent thermal behavior in high-irradiance climates.

The predictive accuracy of PVsyst, when calibrated with orientation-specific U values, is confirmed by the strong correlation between the simulated and experimental energy yields, as demonstrated by the mean bias difference (MBD) and absolute difference remaining below 0.3%, as well as the root mean square difference (RMSD) of less than 5%. This study introduces a validated method for optimizing simulations of monocrystalline silicon BIPV façades, offering researchers and engineers in the Gulf Region and other hot climates effective tools to improve energy efficiency and thermal performance in solar-integrated building designs.

These findings can be further investigated in several valuable ways in future studies. A more comprehensive understanding of the thermal and energy performance across different BIPV technologies could involve examining the effects of various photovoltaic materials, such as thin films, CIGS, or polycrystalline silicon, on the U parameter. The inclusion of additional façade orientations (Southeast and Southwest) in the analysis or the use of other advanced simulation tools could reveal significant differences in modeling methodology and accuracy, ultimately leading to improved methods for assessing BIPV systems. Future research should also explore the influence of wind speed on the electrical and thermal behavior of ventilated BIPV façades, as measured by the wind-dependent heat loss factor (Uv).

ACKNOWLEDGEMENT

This work was funded by the Dubai Electricity and Water Authority (DEWA) under the project "Performance Verification of Advanced Building Integrated Photovoltaics (BIPV) in the UAE." The authors would like to acknowledge the valuable input and support of Sgouris Sgouridis, Director of Research in DEWA R&D.

REFERENCES

[1] Solar resource maps & GIS data for 200+ countries | Solargis. Https://SolargisCom/Resources/Free-Maps-and-Gis-Data n.d.

[2] Quddus AS, Usmani T, Hasan SH. Analysis and Comparison of Energy Generation from a 38.4 kWp BIPV System Using PVsyst Simulation Tool. Indian J Sci Technol 2024;17:5046–54. https://doi.org/10.17485/IJST/v17i48.3772.

[3] Jing Yang R, Zhao Y, Dev Sureshkumar Jayakumari S, Schneider A, Prithivi Rajan S, Leloux J, et al. Digitalising BIPV energy simulation: A cross tool investigation. Energy Build 2024;318. https://doi.org/10.1016/j.enbuild.2024.114484.

[4] Zhao K, Gou Z. Optimizing semi-transparent BIPV windows for balanced daylighting and solar energy performance in office buildings. Solar Energy 2025;287. https://doi.org/10.1016/j.solener.2024.113229.

[5] Khele I, Szabó M. A review of the effect of semi-transparent building-integrated photovoltaics on the visual comfort indoors. Developments in the Built Environment 2024;17. https://doi.org/10.1016/j.dibe.2024.100369.

[6] Romaní J, Ramos A, Salom J. Review of Transparent and Semi-Transparent Building-Integrated Photovoltaics for Fenestration Application Modeling in Building Simulations. Energies (Basel) 2022;15. https://doi.org/10.3390/en15093286.

[7] Lau SK, Zhao Y, Shabunko V, Chao Y, Lau SSY, Tablada A, et al. Optimization and evaluation of naturally ventilated BIPV Façade design. Energy Procedia, vol. 150, Elsevier Ltd; 2018, p. 87–93. https://doi.org/10.1016/j.egypro.2018.09.003.

[8] Martín-Chivelet N, Gutiérrez JC, Alonso-Abella M, Chenlo F, Cuenca J. Building retrofit with photovoltaics: Construction and performance of a BIPV ventilated façade. Energies (Basel) 2018;11. https://doi.org/10.3390/en11071719.

[9] Alhammadi N, Rodriguez-Ubinas E, Alzarouni S, Alantali M. Building-integrated photovoltaics in hot climates: Experimental study of CIGS and c-Si modules in BIPV ventilated façades. Energy Convers Manag 2022;274. https://doi.org/10.1016/j.enconman.2022.116408.

[10] Hasan K, Yousuf SB, Tushar MSHK, Das BK, Das P, Islam MS. Effects of different environmental and operational factors on the PV performance: A comprehensive review. Energy Sci Eng 2022;10:656–75. https://doi.org/10.1002/ese3.1043.

[11] Array Thermal losses. Https://WwwPvsystCom/Help-Pvsyst7/Thermal_lossHtm n.d.

[12] Owen M, Pretorius J, Buitendag B, Nel C. Heat Dissipation Factors for Building-Attached Pv Modules. SSRN Electronic Journal 2022. https://doi.org/10.2139/ssrn.4119337.

[13] Sun C, Lu Y, Ju X. Experimental and numerical study to optimize building integrated photovoltaic (BIPV) roof structure. Energy Build 2024;309. https://doi.org/10.1016/j.enbuild.2024.114070.
[14] Gonçalves JE, van Hooff T, Saelens D. Simulating building integrated photovoltaic façades: Comparison to experimental data and evaluation of modelling complexity. Appl Energy 2021;281. https://doi.org/10.1016/j.apenergy.2020.116032.
[15] Ghabuzyan L, Pan K, Fatahi A, Kuo J, Baldus-Jeursen C. Thermal effects on photovoltaic array performance: Experimentation, modeling, and simulation. Applied Sciences (Switzerland) 2021;11:1–15. https://doi.org/10.3390/app11041460.
[16] Martín-Chivelet N, Polo J, Sanz-Saiz C, Núñez Benítez LT, Alonso-Abella M, Cuenca J. Assessment of PV Module Temperature Models for Building-Integrated Photovoltaics (BIPV). Sustainability (Switzerland) 2022;14. https://doi.org/10.3390/su14031500.
[17] Barykina E, Hammer A. Modeling of photovoltaic module temperature using Faiman model: Sensitivity analysis for different climates. Solar Energy 2017;146:401–16. https://doi.org/10.1016/j.solener.2017.03.002.
[18] Design and simulation software for your photovoltaic systems. Https://WwwPvsystCom/ n.d.
[19] Hamzah AH, Go YI. Design and assessment of building integrated PV (BIPV) system towards net zero energy building for tropical climate. E-Prime - Advances in Electrical Engineering, Electronics and Energy 2023;3. https://doi.org/10.1016/j.prime.2022.100105.
[20] Gomes MM de M, Cavalcante RDL da S, Ando Junior OH, Pero C Del, Lima JA de, Lago TGS do. The Effect of Façade Orientation on the Electrical Performance of a BIPV System: A Case Study in João Pessoa, Brazil. Energies (Basel) 2025;18. https://doi.org/10.3390/en18040829.
[21] Asiri J, Salem N. Building Integrated Photovoltaic, BIPV, System: Design and Simulation for an Educational Building. 2023 13th International Conference on Power, Energy and Electrical Engineering, CPEEE 2023, Institute of Electrical and Electronics Engineers Inc.; 2023, p. 470–9. https://doi.org/10.1109/CPEEE56777.2023.10217764.
[22] Zomer C, Custódio I, Antoniolli A, Rüther R. Performance assessment of partially shaded building-integrated photovoltaic (BIPV) systems in a positive-energy solar energy laboratory building: Architecture perspectives. Solar Energy 2020;211:879–96. https://doi.org/10.1016/j.solener.2020.10.026.
[23] Electricity yield simulation of complex BIPV systems. n.d.
[24] Myong SY, Jeon SW. Efficient outdoor performance of esthetic bifacial a-Si: H semi-transparent PV modules. Appl Energy 2016;164:312–20. https://doi.org/10.1016/j.apenergy.2015.11.063.
[25] Assoa YB, Mongibello L, Carr A, Kubicek B, Machado M, Merten J, et al. Thermal analysis of a BIPV system by various modelling approaches. Solar Energy 2017;155:1289–99. https://doi.org/10.1016/j.solener.2017.07.066.
[26] Edifon AI, Edwin NI, Macaulay EU. Comparative Analysis of the Performance of Different Photovoltaic (PV) Technologies Based on PVSyst Thermal Model. Science Journal of Energy Engineering 2016.